

25, 1261 (1970).

²K. W. Gentle and A. Malein, *Phys. Rev. Lett.* **26**, 625 (1971).

³H. Ikezi and Y. Kiwamoto, *Phys. Rev. Lett.* **27**, 718 (1971).

⁴M. Guillemot, J. Olivain, F. Perceval, and J. Schar-

er, *Phys. Fluids* **14**, 952 (1971).

⁵T. H. Dupree, *Phys. Fluids* **9**, 1773 (1966).

⁶T. H. Jensen, *Phys. Fluids* **13**, 1778 (1970).

⁷A. A. Galeev, V. I. Karpman, and R. Z. Sagdeev, *Dokl. Akad. Nauk SSSR* **157**, 1088 (1964) [*Sov. Phys. Dokl.* **9**, 681 (1965)].

Stochastic Acceleration by a Single Wave in a Magnetic Field

Gary R. Smith and Allan N. Kaufman

Department of Physics and Lawrence Berkeley Laboratory, University of California, Berkeley, California 94720

(Received 10 February 1975)

The nature of a particle orbit in an electrostatic plasma wave is modified by a magnetostatic field, because there exists a set of resonant parallel velocities $(\omega + l\Omega)/k_z$. If the wave amplitude Φ_0 is sufficiently large, neighboring resonant regions overlap, and the particle motion becomes stochastic; the threshold condition is $k_z^2 (e/m)\Phi_0 |J_l(k_\perp \rho)| \approx \Omega^2/16$. As an application, a weakly damped intermediate-frequency ion-acoustic wave may be used to heat the tail of an ion distribution.

The character of the resonant interaction of a particle with an electrostatic wave can be qualitatively different in the presence or absence of an ambient magnetostatic field. In its absence, it is well known¹ that particles whose velocity (projected along the wave vector) differs from the wave phase velocity ω/k by less than the trapping half-width $2(e\Phi_0/m)^{1/2}$ may be trapped into orbits oscillating about the phase velocity at a bounce frequency $k(e\Phi_0/m)^{1/2}$. This behavior, whose short-term consequence is Landau damping, asymptotically limits the net damping and energy (or momentum) transfer of the wave to the resonant particles.

In a magnetized plasma, an electrostatic wave propagating at an oblique angle $\theta = \tan^{-1}(k_\perp/k_z)$ to the uniform field $B_0\hat{z}$ has a set of resonant parallel velocities $\{V_l\}$ which satisfy

$$\omega - k_z V_l = -l\Omega, \quad l=0, \pm 1, \pm 2, \dots, \quad (1)$$

where the left-hand side is the Doppler-shifted wave frequency and the right-hand side is a multiple of the gyrofrequency $\Omega = eB_0/mc$. As shown below, the trapping half-width at the l th resonance is

$$w_l \equiv 2|e\Phi_0 J_l(k_\perp \rho)/m|^{1/2}, \quad (2)$$

where ρ is the gyroradius of the particle. When the wave amplitude Φ_0 is so large that the trapping layers ($V_l \pm w_l$) overlap, a particle can move from one resonance region to the next, executing a random walk in v_z space, so to speak. As a

result, the mean net momentum transfer to the particles can be appreciably larger than expression (2) would indicate. In this paper we study the transition from "adiabatic"² particle trajectories, when Φ_0 is small, to "stochastic" trajectories, when Φ_0 is large. The motion of a particle in a magnetic field and a single oblique wave has previously been treated by Fredricks.³ Analogous studies on cyclotron heating in a mirror field⁴ and on "super-adiabaticity"⁵ may be mentioned.

In the wave frame, moving at $(\omega/k_z)\hat{z}$ with respect to the plasma, the particle Hamiltonian is

$$H(\vec{r}, \vec{p}) = (\vec{p} - m\Omega \times \hat{y})^2/2m + e\Phi_0 \sin(k_z z + k_\perp x).$$

Two canonical transformations allow us to write the Hamiltonian as

$$H(z, p_z; \varphi, p_\varphi) = p_z^2/2m + \Omega p_\varphi + e\Phi_0 \sin(k_z z - k_\perp \rho \sin \varphi), \quad (3)$$

where $p_\varphi = mv_\perp^2/2\Omega$ is the canonical angular momentum of gyration, conjugate to the gyrophase φ , and $\rho \equiv (2p_\varphi/m\Omega)^{1/2}$ is the gyroradius. This Hamiltonian system has two degrees of freedom. Since (3) is independent of time, in the wave frame the energy of the particle is conserved.

To analyze (3), it is helpful to use a Bessel-function identity to write (3) as

$$H = p_z^2/2m + \Omega p_\varphi + e\Phi_0 \sum_l J_l(k_\perp \rho) \sin(k_z z - l\varphi). \quad (4)$$

If the wave amplitude is small enough, we can treat the last term in (4) as a small perturbation δH of the unperturbed Hamiltonian $H_0 = p_z^2/2m + \Omega p_\varphi$. The zeroth-order equations of motion yield $v_z \equiv \dot{z} = p_z/m$, $\dot{\varphi} = \Omega$, $p_z = \text{const}$, $p_\varphi = \text{const}$. Substituting $z = v_z t + z_0$ and $\varphi = \Omega t$ in the last term of (4) yields

$$\delta H \approx e\Phi_0 \sum_l J_l \sin[(k_z v_z - l\Omega)t + k_z z_0].$$

When one of the resonance conditions

$$k_z v_z - l\Omega \approx 0 \tag{5}$$

is satisfied, the motion is dominated by a *single* term of the sum over l for times much longer than Ω^{-1} . [Note that $\omega = 0$ in the wave frame, so (5) is the same condition as (1).] The exact Hamiltonian (4) can then be approximated by

$$H_1 \approx H_0 + e\Phi_0 J_l \sin(k_z z - l\varphi), \tag{6}$$

for which a constant of the motion (in addition to the energy) exists: $I_l \equiv p_\varphi + l p_z/k_z$. When the wave amplitude is *not* small, the above analysis breaks down, and we might expect no additional constant of the motion to exist. By using the exact Hamiltonian (3) we have found that the constant of the motion does indeed disappear fairly abruptly as the wave amplitude increases.

To visualize the disappearance of the constant of the motion we use the "surface-of-section" method. (This method has been used to analyze several other nonlinear oscillator systems.⁶ For present purposes, we view it as a technique for representing the four-dimensional phase-space trajectory in two dimensions.) To construct the surface-of-section plots, the trajectory is calculated numerically using the Hamiltonian equations. We look at a cross section ($\varphi = \pi$) of phase space, and see the trajectory represented by dots in a three-dimensional space. We then project the dots onto a two-dimensional surface. The sample plot in Fig. 1(a) was generated using Hamiltonian (3). In this case the dots, which represent the coordinates of the particle at intervals of the gyroperiod, are projected onto the $z p_z$ plane. In some regions of the plane, which we call adiabatic, initial conditions lead to dots lying on a curve, indicating an additional constant of the motion. In the other regions of the plane, which we call stochastic, initial conditions lead to dots filling an area, indicating that energy is the only constant.

The condition for the onset of stochastic particle motion can be derived using the method of

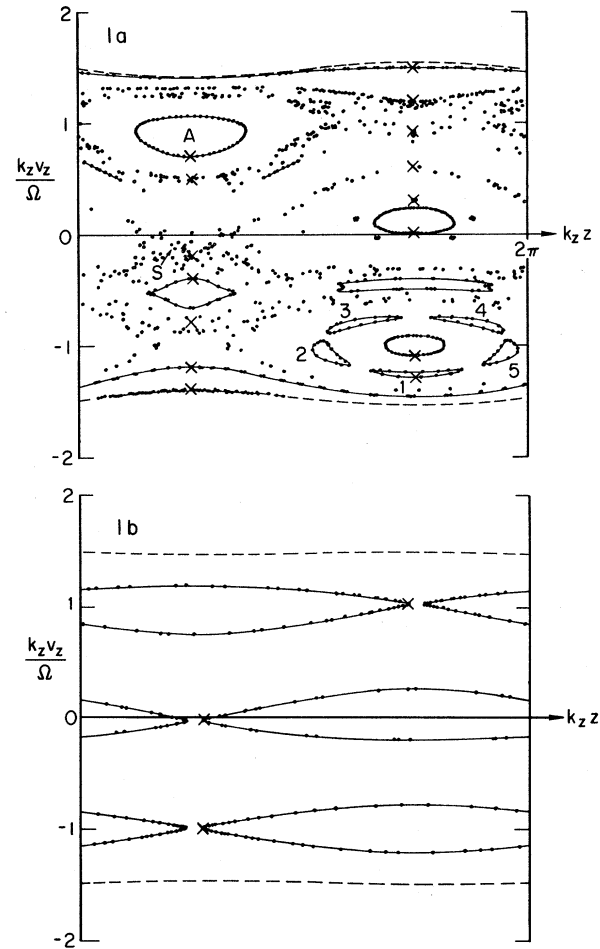


FIG. 1. (a) Sample surface-of-section plot. The A indicates one of the adiabatic regions; S one of the stochastic regions. Curves have been drawn to connect the dots lying in adiabatic regions. The dashed lines represent the limitations on the particle motion due to conservation of energy in the wave frame. The parameters have the fixed values $k_{\perp} \rho_E \equiv k_{\perp} (2E/m)^{1/2} / \Omega = 1.48$, $(\tilde{\omega} / \Omega)^2 \equiv k_z^2 |e\Phi_0| / m\Omega^2 = 0.1$, $\theta = 45^\circ$. The fifteen initial conditions used to generate the dots are shown by crosses. A chain of five islands is indicated by the numbers 1-5. (b) Surface-of-section plot resulting from initial conditions near the three accessible resonances, $l = 0, \pm 1$. The parameters have the same values as in (a) except $(\tilde{\omega} / \Omega)^2 = 0.025$.

Walker and Ford.⁷ We refer to the plot shown in Fig. 1(b), for which the wave amplitude is smaller than for Fig. 1(a), and all initial conditions lead to adiabatic particle motion. Notice the similarity in appearance of each of the three curves to the phase-space orbit of a trapped particle in an unmagnetized plasma.¹ In the magnetized case, the curves shown in Fig. 1(b) are

near the separatrices which surround the resonance conditions (5) for $l=0, \pm 1$. From (6), we see that the trapping half-widths are given by (2). As the wave amplitude increases, these widths increase. The additional constant of the motion will cease to exist, and particle motion will change from adiabatic to stochastic, when two separatrices touch. We may then expect the particle to be able to move from the vicinity of one resonance to the vicinity of another. This occurs when $(w_{i+1} + w_i)$, the sum of neighboring half-widths, equals the resonance separation $|V_{i+1} - V_i| = \Omega/k_z$; i.e., roughly when $(\omega_i/\Omega)^2 \approx \frac{1}{16}$, where $\omega_i \equiv k_z w_i/2$ is the bounce frequency at the i th resonance. This crude estimate is in good agreement with our numerical results, as discussed below.

When the wave amplitude is large enough that particle motion is stochastic, the particle distribution may be significantly heated by the interactions with the wave. The evolution of the distribution resembles a diffusion process in velocity space. These results are illustrated in Fig. 2, which shows two plots for different wave amplitudes. In these plots the trajectory dots have been projected onto the $v_\perp v_z$ plane instead of the $z\rho$ plane. Eight initial conditions were used to generate each of the plots: The initial conditions

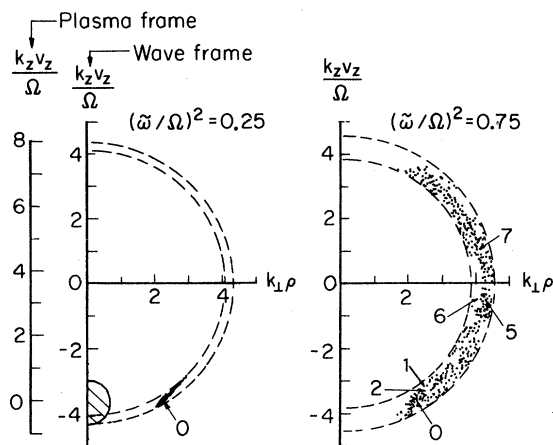


FIG. 2. Two surface-of-section plots illustrating the transition from adiabatic to stochastic particle motion and the onset of heating as the wave amplitude is increased. The values of $(\tilde{\omega}/\Omega)^2$ are shown; the energy parameter has the value $k_\perp \rho_E = 4.24$ and $\theta = 45^\circ$. The axis showing v_z in the plasma frame is based on $\omega = 3.6\Omega$. (a) Cross hatching shows the extent of the thermal ions considered in the wave-heating example. (b) The numbers 0, 1, 2, 5, 6, 7 show the coordinates of the particle initially and at the ends of the corresponding gyroperiods.

all have the same values of the velocity ($k_z v_{\perp 0}/\Omega = k_\perp \rho_0 = 2.24$, $k_z v_{z 0}/\Omega = -3.6$) and gyrophase ($\varphi_0 = \pi$), but different values of z_0 . This set of initial conditions corresponds to ring distribution (in the plasma frame) $\delta(v_z)\delta(v_\perp - v_{\perp 0})$ when $\omega = 3.6\Omega$. In the case of small wave amplitude [$(\tilde{\omega}/\Omega)^2 \equiv k_z^2 |e\Phi_0|/m\Omega^2 = 0.25$], all initial conditions led to adiabatic motion; the velocity of a particle changed little from its initial value. In the case of large wave amplitude [$(\tilde{\omega}/\Omega)^2 = 0.75$], all initial conditions led to stochastic particle motion, and the time-averaged values of both perpendicular and parallel velocities (in the plasma frame) increased significantly.⁸ The transition from adiabatic to stochastic motion corresponds to an increase of wave amplitude by a factor of 3. Our results indicate the transition at about $(\tilde{\omega}/\Omega)^2 = 0.50$. In order to compare this result to the condition $(\omega_i/\Omega)^2 = \frac{1}{16}$, we use $l = -3$ because $k_z v_{z 0}/\Omega = -3.6$ is between the resonances $l = -3$ and -4 , and for the parameters of Fig. 2 the half-width w_{-3} is several times w_{-4} . The numerically observed threshold condition is thus $(\omega_i/\Omega)^2 = (\tilde{\omega}/\Omega)^2 |J_l(k_\perp \rho)| = (0.50) |J_{-3}(2.24)| \approx \frac{1}{12}$, which is remarkably close to $\frac{1}{16}$, considering the crude theory used.

To illustrate the application of these concepts, we choose a particular wave, the intermediate-frequency acoustic⁹ wave, propagating at $\theta = 45^\circ$. This longitudinal wave has the dispersion relation $\omega \approx kc_s$, very similar to an ion-acoustic wave in an unmagnetized plasma. To be specific (and consistent with Fig. 2) we choose $\omega = 3.6\Omega$ and $T_e/T_i = 16$. For these parameters there is negligible linear ion-cyclotron-harmonic damping. We now examine ions in the Maxwell tail, specifically at $v_z = 0$ (in the plasma frame) and $k_\perp \rho = 2.29$ [$v_\perp \approx 3.8(T_i/m)^{1/2}$], which are just the initial conditions used in Fig. 2. These ions will be accelerated by the wave when $(\tilde{\omega}/\Omega)^2 \geq 0.50$, that is, when $e\Phi_0 \gtrsim \frac{3}{2}T_i$. An acoustic wave with $e\Phi_0 = \frac{3}{2}T_i = \frac{1}{11}T_e$ has a density amplitude $\delta n/n \approx \frac{1}{13}$ and a wave-energy density $\omega(\partial\epsilon/\partial\omega)\langle E^2 \rangle/8\pi \approx nT_i/15$, and is thus in the linear regime. We have shown the possibility of heating the tail of the ion distribution by an intermediate-frequency acoustic wave of frequency a few times the gyrofrequency, propagating at an oblique angle, and of a certain minimum amplitude.

We acknowledge useful discussions with S. Johnston, D. Nicholson, B. Cohen, M. Mostrom, C. Birdsall, J. Harte, W. Nevins, A. Lichtenberg, and G. Johnston. This work was supported in part by the U. S. Atomic Energy Commission

and by a National Science Foundation Graduate Fellowship held by one of the authors (G.R.S.).

¹T. M. O'Neil, *Phys. Fluids* **8**, 2255 (1965).

²The terms adiabatic and stochastic have come into use to characterize phase-space orbits that are respectively stable or unstable with respect to an infinitesimal variation of initial conditions. We avoid the term ergodic for an unstable orbit, as the orbit does not fill the whole energy hypersurface, but only a part of it.

³R. W. Fredricks, *J. Plasma Phys.* **1**, 241 (1967). That paper used different methods and obtained different results.

⁴F. Jaeger, A. J. Lichtenberg, and M. A. Lieberman, *Plasma Phys.* **14**, 317 (1972).

⁵R. E. Aamodt, *Phys. Rev. Lett.* **27**, 135 (1971);

M. N. Rosenbluth, *Phys. Rev. Lett.* **29**, 408 (1972); A. V. Timofeev, *Nucl. Fusion* **14**, 165 (1974).

⁶See references in G. M. Zaslavskii and B. V. Chirikov, *Usp. Fiz. Nauk* **105**, 3 (1971) [*Sov. Phys. Usp.* **14**, 549 (1972)]; J. Ford, *Advan. Chem. Phys.* **24**, 155 (1973).

⁷G. H. Walker and J. Ford, *Phys. Rev.* **188**, 416 (1969).

⁸It is clear from Fig. 2 that the particle kinetic energy is essentially constant in the wave frame, while it is increasing in the plasma frame. The increase in parallel kinetic energy (in the plasma frame) is in large part represented by an acceleration of the mean parallel velocity of the affected particles from zero in the plasma frame to zero in the wave frame.

⁹T. E. Stringer, *Plasma Phys.* **5**, 89 (1963); A. B. Mikhailovskii, *Theory of Plasma Instabilities* (Consultants Bureau, New York, 1974), Vol. I, Chap. 8, p. 148.

Nonlinear Evolution of Stimulated Raman Backscatter in Cold Homogeneous Plasma

Paul Koch and James Albritton

Laboratory for Laser Energetics, College of Engineering and Applied Sciences, University of Rochester, Rochester, New York 14627

(Received 24 February 1975)

We present an analytic solution for Raman backscatter in a cold homogeneous plasma, valid until saturation by breaking of the longitudinal waves, or by self-consistent depletion of the pump. We give quantitative values for the pump strength necessary for the former to occur first, and the transmission at saturation. Nonlinear particle bunching causes growth of electromagnetic sidebands. In quarter-critical plasma, a sideband at $\omega = \frac{3}{2}\omega_0$ reaches 8% of the pump intensity at wave breaking.

Two phenomena of the radiation-plasma interaction, beat heating¹⁻³ and the stimulated-Raman-scattering (SRS)⁴⁻⁹ instability, are based on resonant excitation of a longitudinal electron mode by the beat between two electromagnetic waves. When the cold-plasma approximation^{6,10,11} is valid, i.e., when the thermal velocity of an electron is smaller than its directed velocity, the excited longitudinal modes are resonant plasma oscillations.¹¹ Using Lagrangian methods,¹⁰⁻¹³ we can then follow the course of these phenomena analytically until wave breaking¹⁰ occurs, thus exposing the physics directly. The analysis fails at that point, but cold-plasma computer simulations⁶ show that growth of SRS stops when the longitudinal waves break. Thus, the analysis is valid until saturation begins.

Here we report some results of a study of Raman backscatter in a cold, infinite homogeneous

plasma. The physical system is shown in Fig. 1: Two counterpropagating electromagnetic waves, one a high-intensity pump at frequency ω_0 [Fig. 1(a)], the other a reflected wave at frequency $\omega_0 - \omega_p$, growing from the noise [Fig. 1(b)], beat, thus exciting, via $\vec{V} \times \vec{B}$ forces in the longitudinal direction [Fig. 1(c)], a resonant oscillation in the ambient plasma. In the course of this oscillation, the electrons undergo a density perturbation Δn , while at the same time they quiver transversely (with velocity v) in the electric field of the electromagnetic waves. The phase of the resulting incremental current $-ev\Delta n$ is such that it resonantly adds energy to the reflected wave at the expense of the pump wave.⁵ As the amplitude of the plasma oscillation increases, the density perturbations steepen nonlinearly [Fig. 1(d)] and the incremental number density contains growing components at all the harmonics of the beat wave.